Available online at www.sciencedirect.com
ScienceDirect
Trans. Nonferrous Met. Soc. China 25(2015) 3921−3927
Transactions of Nonferrous Metals Society of China
www.tnmsc.cn

Effect of aging time on corrosion behavior of as-forged AZ80 magnesium alloy

Hui-juan LIAO[1], Xiao-feng ZHOU[1], Hui-zhong LI[1,2,3], Min DENG[1], Xiao-peng LIANG[1], Ruo-mei LIU[1]

1. School of Materials Science and Engineering, Central South University, Changsha 410083, China;
2. State Key Laboratory of Powder Metallurgy, Central South University, Changsha 410083, China;
3. Key Laboratory of Nonferrous Metal Materials Science and Engineering of Ministry of Education, Central South University, Changsha 410083, China

Received 24 March 2015; accepted 28 September 2015

Abstract: The corrosion behaviors of an as-forged AZ80 magnesium alloy after aging treatment for various durations at 170 °C were investigated by immersion test, H_2 evolution test, SEM and potentiodynamic polarization curve measurement. The results show that the corrosion rate of the alloy decreases dramatically with the increase of aging time during the initial aging stage, but increases slowly with the aging time longer than 20 h. The volume fraction of β-$Mg_{17}Al_{12}$ increases with aging time within the first 20 h, leading to the decrease of corrosion rate. After aging for longer than 39 h, the growth of β phase is accompanied by the consumption of aluminum in the matrix, resulting in an increase in the corrosion rate. When the volume fraction of β phase is low, specimens suffer from severe local corrosion, which results in a porous surface. On the contrary, when the volume fraction of β phase is high, specimens suffer uniform corrosion attack.

Key words: AZ80 magnesium alloy; aging treatment; corrosion

1 Introduction

Magnesium alloys have been used in aerospace, automobile and electronic products due to its low density, high specific strength and good castability [1,2]. However, the poor corrosion resistance of magnesium alloys restricts their use in corrosive environment. The influence of microstructure on the corrosion resistance of magnesium alloys has been widely reported [3−6]. The β-$Mg_{17}Al_{12}$ phase of magnesium−aluminum-based alloys could play a dual role in the corrosion behavior. It can act as either a galvanic cathode which accelerates the corrosion rate of the matrix, or a kinetic barrier which slows down the corrosion rate of the matrix [7,8]. A stable layer of rich aluminum passivation membrane can easily generate on the surface of β phase, which was inert to corrosion. Reasonable β phases distribution can block matrix corrosion. According to the study of SONG et al [8−10], the β-$Mg_{17}Al_{12}$ phase is expected to act as a barrier under following conditions: the grain size is small, the β phase fraction is not too low and the β phase is nearly continuous over the matrix. On the contrary, β phase is expected to act as a galvanic cathode when the grain size is large, the β phase is agglomerated and the distance between the β phases is large.

Aging treatment can influence the amount and distribution of β phase [11]. LI et al [12] reported that the mechanical properties of AZ80 magnesium alloy could be improved effectively by aging treatment, at an optimum aging temperature of 170 °C. Microstructure evolution will happen concurrently with aging treatment. The microstructure development will undoubtedly influence the corrosion behavior of the alloy. However, there were few studies about the effects of aging treatment on the corrosion behavior of as-forged AZ80 alloy.

In the present study, the corrosion behaviors of as-forged AZ80 magnesium alloy aged at 170 °C for various time were investigated by immersion test, H_2 evolution test, SEM and potentiodynamic polarization curve measurement. The effect of aging time on corrosion behavior of the alloy was discussed.

2 Experimental

2.1 Specimens

The chemical composition of the AZ80 magnesium

Corresponding author: Hui-zhong LI; Tel: +86-731-88830377; Fax: +86-731-88830257; E-mail: lhz606@csu.edu.cn
DOI: 10.1016/S1003-6326(15)64039-0

alloy used in this work are listed in Table 1. The AZ80 specimens were cut from a forged ingot in concentric circles to ensure same property and followed by aging treatment. Aging treatment of as-forged specimens were carried out at 170 °C for 3, 12, 20, 39 and 72 h respectively followed by air cooling.

Table 1 Composition of as-forged AZ80 magnesium alloy (mass fraction, %)

Al	Zn	Mn	Si	Cu	Fe	Mg
8.3	0.46	0.22	≤0.1	≤0.05	≤0.005	Bal.

2.2 Structural characterization

A Sirion 200 scanning electron microscope (SEM) with energy dispersive spectrometer (EDS) was used to analyze the microstructures of all the specimens. Macrostructure of the corroded surfaces after immersion test was pictured by Canon ixus 150 digital camera.

2.3 Corrosion rate measurement

In order to evaluate corrosion rate of all the specimens, immersion tests were carried out in 3.5% NaCl solution for 4 d at ambient temperature of (25±2) °C. The ratio of the solution volume to specimen surface was about 25:1. The solution was unattended during the immersion test. The H_2 collection apparatus is composed of a wide-mouth bottle, a rubber plug and a pipette. With cathodic reaction proceeding, the hydrogen pressure at the solution container would press the solution from the solution container to the pipette, and result in the promotion of liquid plane in the pipette. Therefore, the hydrogen volume produced during the corrosion process of as-forged AZ80 alloy could be recorded with the decay time. Specimens for immersion test were cut into plates of 5 mm in thickness and 30 mm in diameter by a wire cutting machine. A hole of 3 mm in diameter was drilled to facilitate suspending specimen during the test. Three replicated specimens were used for immersion test. Before immersion test, specimens were polished with emery paper followed by acetone cleaning, distilled water cleaning and air drying. After air drying, the specimens were weighed (m_0) before immersion test. The H_2 collection apparatus was used to collect H_2 evolution volume during immersion test. After immersion test, the corroded specimens were immersed in chromate acid (200 g/L CrO_3 + 10 g/L $AgNO_3$) at ambient temperature for 5−8 min to remove the corrosion products. Followed by washing and drying, the specimens were weighed for the final mass (m_1). The values of corrosion rate (R) were calculated using Eq. (1) [13]:

$$R=\frac{(m_0-m_1)}{At} \tag{1}$$

where A is the surface area of specimen and t is the exposure time.

Polarization curves of the specimens were measured in an electrolytic cell, which contained 3.5% NaCl solution as testing solution, using a CS310 electrochemical measurement system. Three-electrode system was used with the as-forged AZ80 magnesium alloy sample as working electrode, platinum as counter electrode, and saturated calomel electrode (SCE) as reference electrode. The polarization started from −1.8 V to −1.3 V by using a scanning rate of 1 mV/s.

3 Results

3.1 Corrosion rate

Figure 1 presents the macro-pictures of samples after immersion in 3.5% NaCl solution for 4 d. It is clear in Fig. 1(a) that as-forged magnesium suffered from severe pitting corrosion. A lot of corrosion cavities can be seen through the enlarged picture of the corroded area of the as-forged specimen. A film of white corrosion products covered the specimen surface. The specimen treated for 3 h presented less pits than the as-forged one, but it also suffered severe local corrosion. Compared with the as-forged and 3 h aging treated specimens, there are no large pitting cavities on the surface of the 12 h aging treated specimen. Compared with the 20 h aging treated specimen, there are some severely corroded areas on the 39 h and 72 h aging treated specimens. Among all the samples, there are few and shallow pitting cavities in 12, 20, 39 and 72 h aging treated specimens, while there are a lot of large, deep pitting cavities in the as-forged and 3 h aging treated specimen.

As shown in the overall magnesium corrosion reaction (Eq. (2)), one molecule of hydrogen is evolved for each atom of corroded magnesium. So, H_2 evolution volume and H_2 evolution velocity (HEV) can reflect the mass loss of corroded magnesium and the magnesium corrosion rate. Measurement of H_2 evolution volume can be a convenient method to make corrosion rate much more visual and dynamic.

$$Mg+H^+ +H_2O=Mg^{2+}+OH^- +H_2 \tag{2}$$

Figure 2 shows the average mass loss of as-forged AZ80 aged at 170 °C for different time after immersing in 3.5% NaCl solution for 4 d. It can be seen in Fig. 2 that corrosion rate of aged magnesium alloys decreases rapidly at first 20 h then increases slowly. And it is clearly seen in Fig. 3 that HEVs of the as-forged and 3 h aging treated specimens accelerate with immersion time. Contrarily, HEVs of the 12, 20, 39 and 72 h aging treated specimens maintain a constant.

3.2 Microstructures

Figure 4 shows the SEM images of the forged AZ80 magnesium alloy and those aged at 170 °C for different

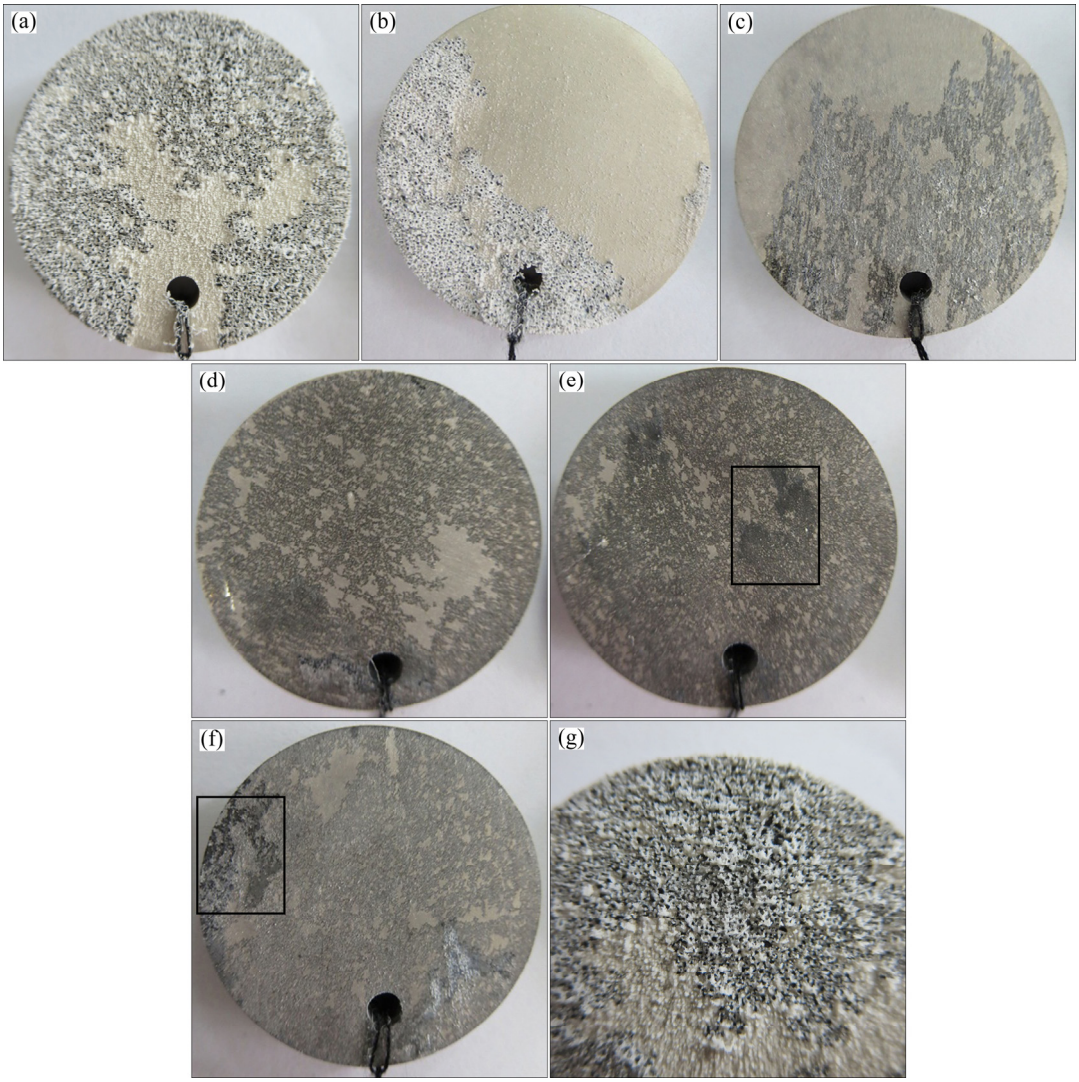

Fig. 1 Macro-pictures of samples after immersion in 3.5% NaCl solution for 4 d: (a) As-forged; (b) Aged for 3 h; (c) Aged-for 12 h; (d) Aged for 20 h; (e) Aged for 39 h; (f) Aged for 72 h; (g) Magnified morphology of (a)

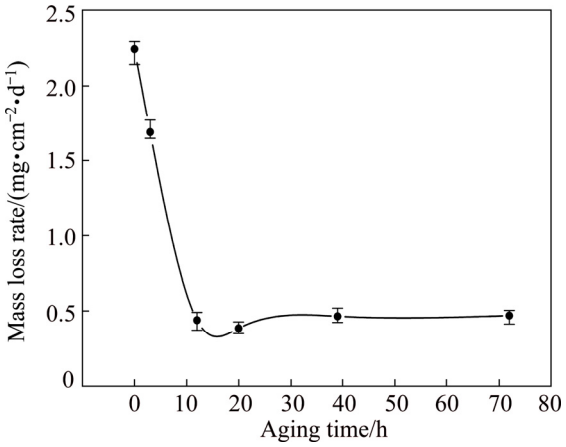

Fig.2 Average mass loss of forged AZ80 aged at 170 °C for different time after immersing in 3.5% NaCl solution for 4 d

time. Few β phases can be seen in the as-forged AZ80 magnesium alloy, and there are large particles along grain boundaries in the as-forged AZ80. The EDS result (Fig. 4(b)) reveals that the chemical compositions are 54.11% Mg, 31.75% Al and 14.14% Mn, it may be Al_6Mn phase.

After aging for 3 h, lamellar β phase precipitated from grain boundary, and grew to inner grain. Compared with the 3 h aging treated specimen, β phase volume fraction of the 12 h aging treated specimen increased remarkably. When aging time increased to 20 h, lamellar precipitate almost occupied the entire grain, and arranged in a certain direction. With aging time increasing, the volume of discontinuous precipitate alone grain boundary does not increase (Fig. 4(g)). And it can be seen in Fig. 4(h) that compared with the 20 h aging treated specimen (Fig. 4(e)), β phase of the 39 h aging treated specimen grew up.

Figure 5 shows the SEM image of the 20 h aging treated specimen after 4 h immersion in 3.5% NaCl solution. There are uniform and compact passivation coatings on the surface protecting matrix from corrosion.

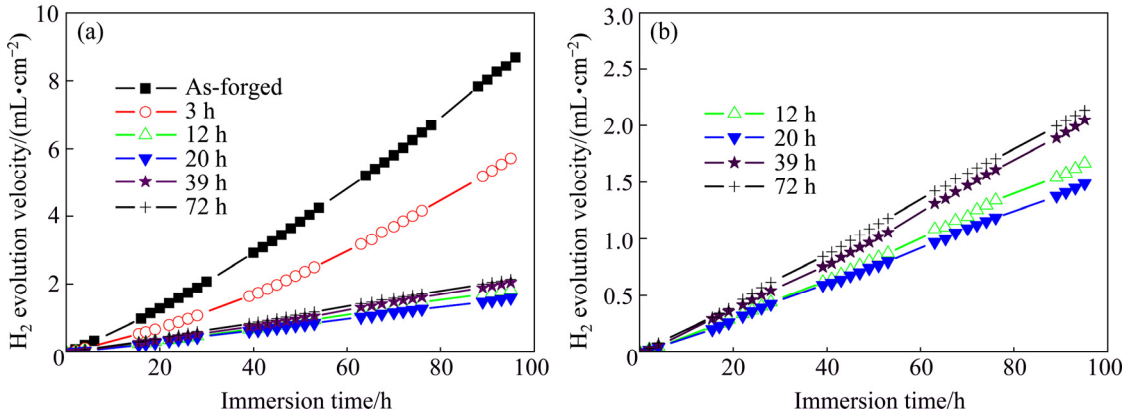

Fig. 3 H_2 evolution velocity of specimens immersed in 3.5% NaCl solution for 4 d: (a) Forged AZ80 aged at 170 °C; (b) Enlarged curves of 12, 20, 39, 72 h aging treated specimens

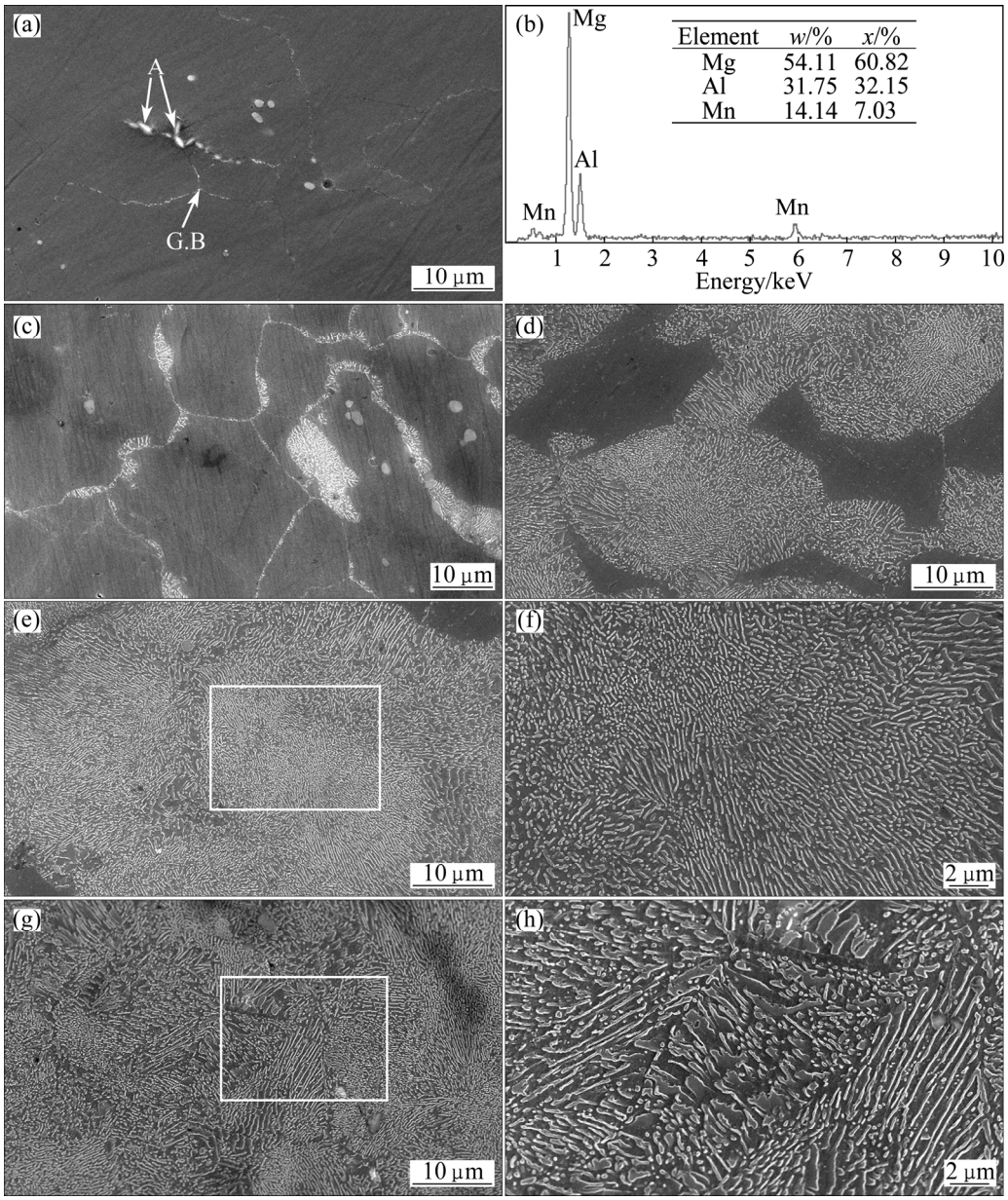

Fig. 4 SEM image of as-forged and aged samples: (a) As-forged; (b) EDS pattern of particle *A* in (a); (c) Aged for 3 h; (d) Aged-for 12 h; (e) Aged for 20 h; (f) Magnified morphology of (e); (g) Aged for 39 h; (h) Magnified morphology of (g)

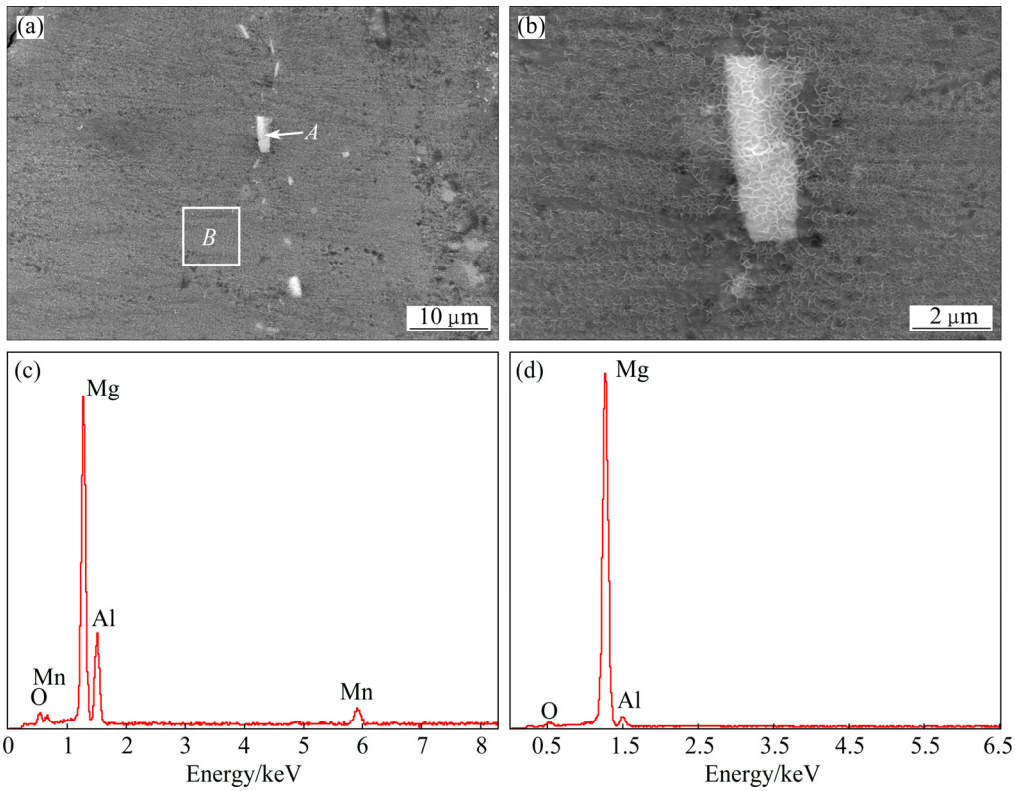

Fig. 5 SEM images and EDS analyses of 20 h aging treated sample after 4 h immersion in 3.5% NaCl solution: (a) SEM image; (b) Enlarged image of (a); (c) EDS pattern of particle *A* in (a); (d) EDS pattern of area *B* in (a)

From Fig. 5(a), particles along grain boundary can be seen. The EDS results (Fig. 5(c)) show that the composition of particle *A* in Fig. 5(a) is 51.92% Mg, 31.36% Al, 10.88% Mn and 5.84% O. And the EDS results (Fig. 5(d)) show the passivation coating of matrix containing 87.38% Mg, 8.83% Al and 3.79% O, which may be a mixture of Al_2O_3 and MgO. AMBAT et al [14] found this two corrosion products in both die-cast and AZ91 magnesium alloy ingots. Particle *A* may be Al_6Mn phase. Because the free corrosion potential of Al_6Mn phase is much higher than that of magnesium [15], Al_6Mn phase easily causes galvanic corrosion in the vicinity of it. It can be seen in Fig. 5(b) that matrix around Al_6Mn phase is corroded while matrix away Al_6Mn phase is protected well by β phase.

3.3 Polarization curve test

Figure 6 suggests that the cathodic polarization current density decreases with aging time within the first 20 h then increases slowly. The cathodic polarization current density of specimen aged for 20 h is much smaller than other specimens. This indicates that the cathodic reaction is increasingly difficult kinetically on specimens when aged for 20 h.

The electrochemical parameters are given in Table 2. The corrosion potential (φ_{corr}) and current density (J_{corr}) were calculated by CView2 software for the cathodic

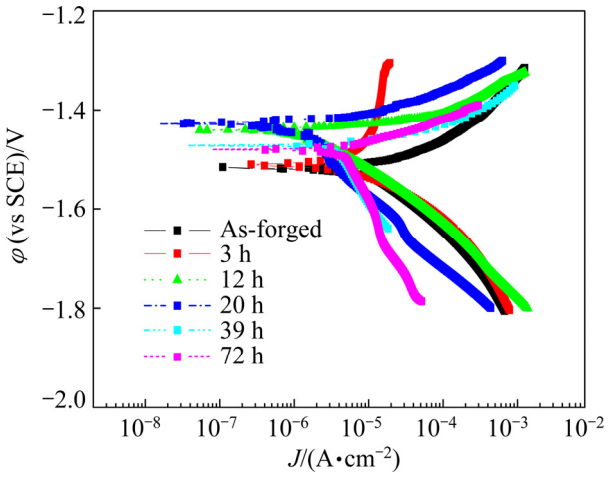

Fig. 6 Polarisation curves of forged AZ80 aged at 170 °C for different time after immersing in 3.5% NaCl solution

Table 2 J_{corr} and φ_{corr} values evaluated from polarization curves

Aging time/h	φ_{corr}/V	J_{corr}/(μA·cm^{-2})
As-forged	−1.5144	128.4
3	−1.5063	87.5
12	−1.441	24.9
20	−1.4286	21.7
39	−1.4694	37.8
72	−1.48	40.2

branches of the polarization curves in Fig. 6. Table 2 reveals that aging treatment retards the corrosion of AZ80. Meanwhile, 20 h aging treated sample presents the lowest corrosion current density.

4 Discussion

The defects such as twins and dislocation in the as-forged specimen can accelerate corrosion [16,17]. Large Al_6Mn particles along grain boundaries caused galvanic corrosion and were detrimental to corrosion resistance. Galvanic corrosion caused by Al_6Mn particles can be seen in Fig. 5(b). As $Mg(OH)_2$, the main corrosion products of magnesium alloys, cannot protect magnesium alloys very well [8], low volume fraction of β phases cannot form effective corrosion barrier, so the as-forged and 3 h aging treated specimens suffered from severe pitting corrosion. In addition, according to the product formation (Eq. (4)) between magnesium ions and hydroxide ions, the hydrogen ions of the dissociated water are left over. This could produce an acid ion on the surface [18,19]. As more magnesium ions go into solution by anodic polarization, more hydroxide ions from dissociated water react with the magnesium ions and stronger water dissociation occurs. Therefore, electrons are consumed by external polarization with the potentiostat and by hydrogen ions from the dissociated water. Then, the dissolution of magnesium increases rapidly. This further disturbs the non-equilibrium of the dissociated water and an increasing hydrogen evolution can be noticed [19]. And this was in correspondence with the accelerated H_2 evolution velocity of the as-forged and 3 h aging treated specimen when immersion time increases.

After aging for 3 h, few lamellar β phases precipitate from grain boundaries (Fig. 4(c)). Increasing the volume of β phase can improve corrosion resistance [8−10], so compared with the as-forged one, the corrosion rate of the 3 h aging treated specimen decreased. Meanwhile, owing to the low volume fraction of β phase, there is very limited barrier effect on improving corrosion resistance. So, the 3 h aging treated specimen showed similar porous structure like the as-forged one, and also suffered severe pitting corrosion.

Figure 4(e) presents precipitate morphologies of the 20 h aging treated specimen. Compared with the 3 h aging treated specimen, β phase volume of the 20 h aging treated specimen remarkably increased, leading to the grain almost occupied by lamellar β phase. It was found that β phase was stable in a wide pH range (4−14) [6]. It can be clearly seen in Fig. 4(f) that spaces between β phases are small. When the α grains are fine and β fraction is not too low, the oxide film formed on β phase is nearly continuous [8]. Continuous and compact oxide film can be seen in Figs. 5(a) and (b). Owing to the presence of fine β phases, there were no large, deep pits in the 20 h aging treated specimen, and relatively uniform corrosion morphology appeared in Fig. 1. In addition, compact oxide film of β phase was more stable than $Mg(OH)_2$. So, compared with the as-forged and 3 h aging treated specimens, HEVs of the 12, 20, 39, 72 h aging treated specimens almost maintained a constant value during 4 d immersion in 3.5% NaCl solution.

With increasing aging time, β phases kept growing accompanied by the consumption of aluminum in the matrix. MATHIEU et al [21] reported that aluminium is benificial to the protection of the α-phases, therefore, the φ_{corr} of AZ91 alloy increases with Al content whereas J_{corr} decreases. Meanwhile, according to the study of AMBATE et al [14], the areas with low aluminum contents are prone to corrosion attack. Similar with the aforementioned results, the current work revealed that compared with the 20 h aging treated specimen, the corrosion rate of the 39 and 72 h aging treated specimens increased slightly.

5 Conclusions

1) Corrosion rate of as-forged magnesium alloys decreases rapidly by aging treatment within first 20 h, then increases slowly with prolonging aging time. H_2 evolution velocities of the as-forged and 3 h aging treated specimens accelerate with immersion time, while those of the 12, 20, 39, 72 h aging treated specimens almost maintain a constant value during 4 d immersion.

2) Dense lamellar precipitates act as barriers and protect matrix from corrosion effectively. When the volume fraction of β phase is low, specimens undergo severe local corrosion and its surface presents porous structure. Contrarily, when volume fraction of β phase is high, specimens suffer uniform corrosion.

References

[1] KULEKCI M K. Magnesium and its alloys applications in automotive industry [J]. The International Journal of Advanced Manufacturing Technology, 2008, 39(9): 851−865.

[2] LI Hui-zhong, WEI Xiao-yan, OUYANG Jie, JIANG Jun, LI Yi. Hot deformation behavior of extruded AZ80 alloy [J]. Transactions of Nonferrous Metals Society of China, 2013, 23(11): 3180−3185.

[3] LI Hui-zhong, LIU Hong-ting, GUO Fei-fei, WANG Hai-jun, LIANG Xiao-peng, LIU Chu-ming. Effect of ageing time on corrosion behavior of Mg−10Gd−4.8Y−0.6Zr extruded-alloy [J]. Transactions of Nonferrous Metals Society of China, 2011, 21(7): 1498−1505.

[4] LIU Xian-bin, SHAN Da-yong, SONG Yi-wei, HAN En-hou. Effects of heat treatment on corrosion behaviors of Mg−3Zn magnesium alloy [J]. Transactions of Nonferrous Metals Society of China, 2010, 20(7): 1345−1350.

[5] BELDJOUDI T, FIAUD C, ROBBIOLA L. Influence of homogenization and artificial aging heat treatments on corrosion

behavior of Mg−Al alloys [J]. Corrosion, 1993, 49(9): 738−745.
[6] LUNDER O, LEIN J E, AUNE T K, NISANCIOGLU K. The role of $Mg_{17}Al_{12}$ phase in the corrosion of Mg alloy AZ91 [J]. Corrosion, 1989, 45(9): 741−748.
[7] ZENG Rong-chang, ZHANG Jin, HUANG Wei-jiu, DIETZEL W, KAINER K U, BLAWERT C, KE W. Review of studies on corrosion of magnesium alloys [J]. Transactions of Nonferrous Metals Society of China, 2006, (S2): s763−s771.
[8] SONG Guang-lin, ATRENS A. Understanding magnesium corrosion —A framework for improved alloy performance [J]. Advanced Engineering Materials, 2003, 5(12): 837−858.
[9] SONG Guang-lin, BOWLES A L, STJOHN D H. Corrosion resistance of aged die cast magnesium alloy AZ91D [J]. Materials Science and Engineering A, 2004, 366(1): 74−86.
[10] SONG Guang-lin, ATRENS A, DARGUSCH M. Influence of microstructure on the corrosion of diecast AZ91D [J]. Corrosion Science, 1999, 41(2): 249−273.
[11] BRASZCYNSKA-MALIK K N. Discontinuous and continuous precipitation in magnesium-aluminium type alloys [J]. Journal of Alloys and Compounds, 2009, 477(1): 870−876.
[12] LI Yan, ZHANG Zhi-min, XUE Yong. Influence of aging on microstructure and mechanical properties of AZ80 and ZK60 magnesium alloys [J]. Transactions of Nonferrous Metals Society of China, 2011, 21(4): 739−744.
[13] ZHOU Wei, SHEN Tian, AUNG N N. Effect of heat treatment on corrosion behaviour of magnesium alloy AZ91D in simulated body fluid [J]. Corrosion Science, 2010, 52(3): 1035−1041.
[14] AMBAT R, AUNG N N, ZHOU W. Evaluation of microstructural effects on corrosion behaviour of AZ91D magnesium alloy [J]. Corrosion Science, 2000, 42(8): 1433−1455.
[15] MERINO M C, PARDO A, ARRABAL R, MERINO S, CASAJAU P, MOHEDANO M. Influence of chloride ion concentration and temperature on the corrosion of Mg−Al alloys in salt fog [J]. Corrosion Science, 2010, 52(5): 1696−1704.
[16] AUNG N N, ZHOU W. Effect of grain size and twins on corrosion behaviour of AZ31B magnesium alloy [J]. Corrosion Science, 2010, 52(2): 589−594.
[17] ZHANG Tao, SHAO Ya-wei, MENG Guo-zhe, CUI Zhong-yu, WANG Fu-hui. Corrosion of hot extrusion AZ91 magnesium alloy: I. Relation between the microstructure and corrosion behavior [J]. Corrosion Science, 2011, 53(5): 1960−1968.
[18] FRANKEL G S. Pitting corrosion of metals a review of the critical factors [J]. Journal of the Electrochemical Society, 1998, 145(6): 2186−2198.
[19] BENDER S, GOWLLNER J, HEYN A, SCHIMIGALLA S. A new theory for the negative difference effect in magnesium corrosion [J]. Materials and Corrosion, 2012, 63(8): 707−712.
[20] PARDO A, MERINO M C, COY A E, ARRABAL R, VIEJJO F, MATYKINA E. Corrosion behaviour of magnesium/aluminium alloys in 3.5wt.% NaCl [J]. Corrosion Science, 2008, 50(3): 823−834.
[21] MATHIEU S, RAPIN C, STEINMETZ J, STEINMETZ P. A corrosion study of the main constituent phases of AZ91 magnesium alloys [J]. Corrosion Science, 2003, 45(12): 2741−2755.

时效时间对锻造 AZ80 镁合金腐蚀性能影响

廖慧娟[1]，周效枫[1]，李慧中[1,2,3]，邓 敏[1]，梁霄鹏[1]，刘若梅[1]

1. 中南大学 材料科学与工程学院，长沙 410083；
2. 中南大学 粉末冶金国家重点实验室，长沙 410083；
3. 中南大学 有色金属材料科学与工程教育部重点实验室，长沙，410083

摘 要：通过浸泡实验、析氢实验、SEM 和极化曲线测试研究在 170 ℃ 下不同时效时间对锻造 AZ80 镁合金腐蚀性能的影响。结果表明：在时效初期阶段，锻造 AZ80 镁合金腐蚀速率随着时效时间的延长而急剧降低，而时效时间超过 20 h 后腐蚀速率又缓慢上升。当时效时间小于 20 h 时，β-$Mg_{17}Al_{12}$ 含量随时效时间的延长不断增加，锻造 AZ80 镁合金腐蚀速率降低；时效 39 h 后，β 相长大，基体中铝含量降低，导致随着时效时间的延长合金腐蚀速率上升。当 β-$Mg_{17}Al_{12}$ 相含量较低时，试样容易产生点蚀，试样表面呈多孔蜂窝状；反之，当 β-$Mg_{17}Al_{12}$ 相含量较高时，试样腐蚀较均匀。

关键词：AZ80 镁合金；时效处理；腐蚀

(Edited by Xiang-qun LI)